Russ. J. Numer. Anal. Math. Modelling, Vol. 27, No. 2, pp. 191–212 (2012)
DOI 10.1515/ rnam-2012-0011

Continuous mathematical model of platelet thrombus formation in blood flow

A. TOKAREV[*], I. SIRAKOV[†], G. PANASENKO[†], V. VOLPERT[‡], E. SHNOL[§], A. BUTYLIN[*¶], and F. ATAULLAKHANOV[*¶||]

Abstract — An injury of a blood vessel requires quick repairing of the wound in order to prevent a loss of blood. This is done by the hemostatic system. The key point of its work is the formation of an aggregate from special blood elements, namely, platelets. The construction of a mathematical model of the formation of a thrombocyte aggregate with an adequate representation of its physical, chemical, and biological processes is an extremely complicated problem. A large size of platelets compared to that of molecules, strong inhomogeneity of their distribution across the blood flow, high shear velocities, the moving boundary of the aggregate, the interdependence of its growth and the blood flux hamper the construction of closed mathematical models convenient for biologists. We propose a new PDE-based model of a thrombocyte aggregate formation. In this model, the movement of its boundary due to the adhesion and detachment of platelets is determined by the level set method. The model takes into account the distribution inhomogeneity of erythrocytes and platelets across the blood flow, the invertible adhesion of platelets, their activation, secretion, and aggregation. The calculation results are in accordance with the experimental data concerning the kinetics of the ADP-evoked growth of a thrombus *in vivo* for different flow velocities. The model constructed here can be easily extended to the case of other hemostatic mechanisms and can be integrated into different continuous blood flow models.

The hemostasis is an evolutionary developed protection system minimizing blood loss in a rupture of the vascular system, i.e., in an injury of the wall of some blood vessel of an organism [12]. The central participants of the hemostasis system are platelets, which are the smallest form elements of the blood having the size about 1 μm. These elements are comparatively few in number, but possess unique properties. Platelets are instantly activated near the injured vascular wall and become capable of strong adhesion to the wall and to each other [31, 45, 52]. Due to this fact, the injured place quickly becomes pasted up with an aggregate of activated platelets, which prevents the loss of blood. The activated platelets produce solu-

[*]National Research Center for Hematology, Ministry of Health and Social Development of Russian Federation, Moscow 125167, Russia. Corresponding author (e-mail: alexey.tokarev@mail.ru).

[†]University Jean Monnet, Saint-Etienne 42023, France

[‡]Institute of Mathematics, University Lyon 1, Villeurbanne 69622, France

[§]Institute of Mathematical Problems of Biology RAS, Pushchino 142290, Moscow Region, Russia

[¶]Faculty of Physics, M. V. Lomonosov Moscow State University, Moscow, Russia

[||]Center for Theoretical Problems of Physicochemical Pharmacology RAS, Moscow 119991, Russia

ble agents, which are activators of platelets brought with the flow. The plasmatic coagulation system works in the gaps between the aggregated platelets where it is protected from the oncoming blood flow. This system governs the formation of the fibrin net fastening the platelets. The hemostatic plug obtained in this process prevents the blood from flowing out of the vessel during the total time of recovery of the injured vascular wall. Since the spatial growth of the thrombocyte aggregate is the key point in the work of the hemostasis system, the main purpose of this paper is the development of a simple continuous mathematical model describing this growth. This model has to be simple in implementation and applied both for the study of the hemostasis regulation and for integration into complex models of blood flow in vessels and vascular networks.

The adhesion of platelets to the injured vascular wall or to the surface of a growing aggregate is a principally nonlocal process, a platelet adheres to the surface only if the distance from its center to the point of fixation is smaller or equal to its size. Therefore, the adhesion rate at a given spatial point is determined by the content of the active surface in some finite neighbourhood of this point. This nonlocal problem can be reduced to integro-differential equations, whose solution is, however, very resource-intensive. Within the framework of the Euler approach, the problem of nonlocality can be solved by introducing a new variable 'sensitive' to the state of the neighbourhood, i.e., the concentration of 'elastic links' between the platelets [19] or the concentration of the virtual short-living substance produced by them and diffusing over a small distance [33]. There is a more general method of tracing the domains interface boundary motion, this is the level set approach (LSA) [2, 38]. It allows one to determine the distance to the boundary by using one additional differential equation (Hamilton–Jacobi equation) describing the boundary movement and joined to other differential equations of the problem. This gives us the ability to distribute the surface processes over the transition zone of a finite length. However, the LSA has not been applied yet to the simulation of the boundary motion occurring due to the adhesion of particles to it. In this paper we use the LSA to determine the motion of the boundary of a thrombocyte aggregate under invertible adhesion of platelets to it.

Another important aspect of hemostasis is the near-wall blood layer concentration with platelets. Platelets are displaced from the core of the blood flow by erythrocytes migrating from the walls to the axis of the flow [1]. Erythrocytes whose mean volume concentration is about 40–45% continuously push each other in the shear blood flow, which results in their regular random movement across the flow, i.e., shear-caused dispersion. The dispersion of platelets causes the dispersion of the surrounding plasma and the platelets contained in it [15, 24, 57]. The dispersive motion is described by the same equations as molecular diffusion. However, the ordinary diffusion equation (the first Fick's law) is unable to describe the spatial distribution inhomogeneity of particles (platelets across the flow in our case) in principle, because it leads to an equalizing of the concentrations. The phenomenological solution to this problem has been obtained by introducing an additional term into this equation. This term is the passive flow oriented towards to wall caused by

the gradient of the 'rheological potential' [16, 17, 56]. Unfortunately, this approach leaves the mechanism of displacement beyond consideration, but the determination of the form of the 'rheological potential' requires *a priori* knowledge of the answer, i.e., the form of the stationary platelets distribution under the given conditions. Naturally, this is impossible in the case of a growing thrombus, which regularly changes the geometry of the flow. Recent theoretical studies show that the concentration of the wall layer is generally determined by the inability of the platelets to take place between the erythrocytes, and the 'rheological potential' may be directly related to the volume fraction physically accessible for platelets in the space between the erythrocytes [13, 50]. In this paper we extend this result to the general case of a flow with a nonuniform transversal distribution of platelets flowing around a growing thrombocyte aggregate.

Thus, in this paper we present the new mathematical model of the growth of a thrombocyte aggregate (thrombus). Its advantages are the equation-based method of determination of the boundary motion (by the level set approach) and the consideration of a nonuniform distribution of platelets and erythrocytes across the flow streamlining the thrombus (by calculation of the distribution of the volume accessible for platelets). Our model consists of a system of linked PDE and can be easily implemented and integrated into other PDE-based models.

1. Mathematical model

We describe all basic processes occurring to a platelet in the blood flow and in the activation zone:

- the transport of platelets along and across the flow;
- the capture of a platelet by the injured vascular wall or by the surface of a thrombocyte aggregate;
- the activation of a platelet by the action of ADP and shear tension;
- release of ADP by an activated platelet;
- detachment of a captured platelet by the flow.

The description of these processes requires simultaneous taking into account of the following factors:

- the transport of platelets in the flow;
- the growth of the aggregate in the flow;
- the obstacle for the blood flow caused by the aggregate.

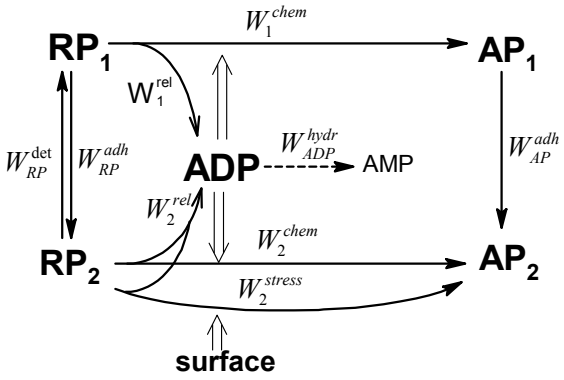

Figure 1. Kinetic scheme of activation and adhesion of platelets. Nonactivated platelets are denoted by RP_1 and RP_2, activated ones — by AP_1 and AP_2. Platelets release ADP in their activation (curved arrows), which activates other platelets (double arrows) and is hydrolyzed with generation of AMP (dotted line). Platelets captured by the surface of the thrombus are also activated by shear tension.

The general kinetic scheme of the described processes is presented in Fig. 1, the differential equations of the model are presented in Appendix A, the values of all the parameters are given in Table 1 below. Depending on their state, platelets are denoted by RP_1, AP_1 (resting and activated platelets in the flow) and RP_2, AP_2 (fixed resting and activated platelets). The volume fraction of erythrocytes is denoted by Φ_{RBC}, the flow velocity is $\bar{u} = (u, v)$, the pressure is p. Below we explain the meaning of all terms of these equations.

1.1. Adhesion and activation of platelets

1.1.1. Adhesion of platelets. The capture of platelets from the blood flow occurs onto the injured part of the vascular wall and onto platelets that have becomes a part of the aggregate but are lying for a while on its surface [31, 45, 52]. The dimension of the boundaries is always less by one than the dimension of the space. Using the LSA, we replace the boundary of the thrombocyte aggregate by a narrow transition zone of the half-thickness s, where the platelets carried by the flow are captured at the rate

$$W_{RP}^{\mathrm{adh}} = \alpha J_{RP}^{\mathrm{wall}} \chi \frac{\Theta}{s}$$
$$W_{AP}^{\mathrm{adh}} = \alpha J_{AP}^{\mathrm{wall}} \chi \frac{\Theta}{s} \tag{1.1}$$

Here α is the capture efficiency, J_{RP}^{wall} and J_{AP}^{wall} are the platelets flows toward the wall. The function Θ is the surface indicator: $\Theta > 0$ in the narrow transition zone where the adhesion occurs and is equal to zero outside of it. We construct Θ so that the ratio $\Theta(r)/s$ tends to the δ-function $\delta(r)$ for $s > 0$ in the direction r per-

Table 1.
Parameters of the model: (a) Typical diameter of arterioles and venules is $20 \div 70$ μm [27,43]; venule diameter in experiment [3] is $40 \div 70$ μm. (b) Found by integration of (1.37). (c) The ADP inflow rate in [3] was $2 \cdot 10^{-14}$ mole/s; the coefficient 10^{24} converts mole/μm^3 to nm. (d) At normal extracellular concentration of Ca^{2+}-ions a platelet releases approximately only 6% of ADP in response to shear tension [35] and to ADP [32].

Parameter	Notation	Value	Notes and references
Sizes of the calculation domain:			
length of the vessel	$L_1 + L_2$	150 μm	
width of the vessel	L_3	50 μm	(a)
width of the additional domain	L_4	10 μm	
initial height of the aggregate	h_0	0	
radius of ADP inflow section on the vessel wall	b	5 μm	
Concentrations:			
mean concentration of platelets in blood	P_0	$429 \cdot 10^{-4}/\mu\text{m}^3$	[3]
mean volume portion of erythrocytes in blood	Φ_D	0.4	[9, 24]
mean cross-section portion of the volume accessible for platelets	$\bar{\Phi}_a$	0.396	(b)
ADP flow through the wall in the activation zone	J_{ADP}	$2 \cdot 10^{-14} \cdot 10^{24}/\pi b^2$ mole·s/μm^2	(c)
Activation of platelets:			
in response to ADP	T_{ADP}	3 s	[21]
	$[ADP]_{1/2}$	2000 nm	
	n_{ADP}	2	
in response to shear tension	T_τ	25 s	[10]
	$\tau_{1/2}$	90 dyne/cm^2	
	n_τ	4	
quantity of ADP contained in a platelet	$\lambda_{\max}$	$3.3 \cdot 10^7$ nm/(pl/μm^3)	[47]
quantity of ADP released from a platelet in its activation	λ_{ADP}	$0.06 \cdot \lambda_{\max}$	(d)
hydrolysis of ADP by nucleotidases in blood	$V_m^{\text{hydr,ADP}}$	80 nm/s	[11]
	$K_m^{\text{hydr,ADP}}$	21700 nm	
coefficient of diffusion of ADP	D_{ADP}	257 μm^2/s	[20, 25, 48]
Adhesion of platelets:			
collision parameter	K	1 μm	estimated from [49]
detachment velocity constant	δ	$4 \cdot 10^{-6}$	estimated from [25]

Table 1.
(continuation) Parameters of the model: (e) Estimated from the mean volume of a platelet V_{RP}=8 μm^3 by the formula $a_{RP} = (3V_{RP}/4\pi)^{1/3}$.

Parameter	Notation	Value	Notes and references
Blood flow:			
blood density	ρ	$1.056 \cdot 10^{-6} ug/\mu\text{m}^3$	[37]
density of blood and plasma	η, η_P	4.5 cP, 1.2 cP	[9,24]
initial near-wall shear velocity	$\dot{\gamma}_{w,0}$	$0 \div 1000$ s^{-1}	see figure legends
Growth of the aggregate:			
platelet equivalent radius	a_{RP}	1.24 μm	(e)
concentration of platelets in the aggregate	P_m	$1/(60\mu\text{m}^3)$	estimated from [5–7]
width of the transition zone	s	2.5 μm	
stabilization of the equation for the level function	λ	2 μm^2/s	
	β	20 s^{-1}	
	w_0	1 μm/s	
coefficient of permeability of the aggregate	K_D	0.61 μm^2	see (1.28)

pendicular to the surface of the aggregate ($r = 0$ on the surface of the aggregate, see equation (1.15) below). The function χ in equation (1.1) indicates the ability of the surface of the aggregate or a vascular wall to fix a platelet. It is assumed that platelets can be captured from the flow either by activated platelets of the growing aggregate (AP_2), or by the injured part of the vascular wall (the domain where $\Theta > 0$ for $t = 0$):

$$\chi = \max\left[\frac{AP_2}{RP_2 + AP_2}, \Theta_{t=0}\right] (p_2 < 1). \tag{1.2}$$

Here p_2 is the total concentration of aggregated platelets normalized by its maximal possible value:

$$p_2 = \frac{RP_2 + AP_2}{P_m}. \tag{1.3}$$

The flow of platelets onto the wall generally occurs due to their near-wall collisions with erythrocytes, the frequency of those collisions is proportional to the product of the shear rate magnitude $\dot{\gamma}$ and the volume fraction of erythrocytes Φ_{RBC} [49]:

$$\begin{aligned} J_{RP}^{\text{wall}} &= K\dot{\gamma}\Phi_{RBC}RP_1 \\ J_{AP}^{\text{wall}} &= K\dot{\gamma}\Phi_{RBC}AP_1. \end{aligned} \tag{1.4}$$

By the definition, for a flow developing in the x-direction we have $\dot{\gamma} = |\partial u/\partial y| \equiv |u_y'|$. The magnitude of the rate-of-strain tensor can be used for the calculation of the particle collision frequency in the general case of a curvilinear flow [28]. In the

two-dimensional case it is calculated from the second invariant of the rate-of-strain tensor by the formula

$$\dot{\gamma} = \sqrt{2u_x'^2 + \left(u_y' + v_x'\right)^2 + 2v_y'^2}. \tag{1.5}$$

1.1.2. Detachment of platelets from the thrombus. Nonactivated platelets form only a temporary contact with the active surface [25,36,55]. The rate of their detachment from the surface, i.e., from the layer with the thickness equal to the diameter $2a_{RP}$ of a platelet is proportional to the shear velocity

$$\tilde{W}_{RP}^{\text{det}} = \delta\,\dot{\gamma} RP_2\,\tilde{\Theta}. \tag{1.6}$$

Here $\tilde{\Theta}$ is the function similar to Θ and equal to 1 on the exact boundary of the aggregate, but with the half-width $2a_{RP}$. Proceeding from $\tilde{\Theta}$ to Θ and keeping the total detachment rate with respect to the cross-section of the transition zone (i.e., the flow from the wall), we get

$$W_{RP}^{\text{det}} = \delta\,\dot{\gamma} RP_2\,\Theta\frac{2a_{RP}}{s}. \tag{1.7}$$

Thus, both adhesion and detachment of nonactivated platelets occur in the transition zone determined by the function Θ.

1.1.3. Activation of platelets under the effect of ADP. The activation of a platelet by different activators occurs in a trigger manner according to the rule '*all or nothing*': low concentrations practically do not influence a platelet, but high ones cause the complete activation in a finite time determined by the nature of its inner signal systems [21, 22, 26, 47, 53]. Therefore, we assume that the activation rate depends on the concentration of ADP according to Hill:

$$\begin{aligned} W_1^{\text{chem}} &= \frac{(ADP/ADP_{1/2})^{n_{ADP}}}{1+(ADP/ADP_{1/2})^{n_{ADP}}}\cdot\frac{RP_1}{T_{\text{ADP}}} \\ W_2^{\text{chem}} &= \frac{(ADP/ADP_{1/2})^{n_{ADP}}}{1+(ADP/ADP_{1/2})^{n_{ADP}}}\cdot\frac{RP_2}{T_{\text{ADP}}} \end{aligned} \tag{1.8}$$

Here n_{ADP} and $ADP_{1/2}$ are parameters, T_{ADP} is the typical activation time for a platelet for the saturating concentration of ADP.

1.1.4. Surface activation of platelets by shear tension. Along with activation by soluble agonists, platelets captured from the flow by the surface can be also activated by the action of shear tension [45]. This response also has a threshold character [10, 27]. Assuming that nonactivated platelets lying in the surface layer with the thickness equal to the diametrical size of a platelet $2a_{RP}$ are subject to

shear tension activation, we write its rate in the form

$$\tilde{W}_2^{\text{stress}} = \frac{(\tau/\tau_{1/2})^{n_\tau}}{1+(\tau/\tau_{1/2})^{n_\tau}} \frac{RP_2}{T_\tau} \tilde{\Theta} \tag{1.9}$$

Passing from $\tilde{\Theta}$ to Θ preserving the total activation rate relative to the cross-section of the transition zone, we get

$$W_2^{\text{stress}} = \frac{(\tau/\tau_{1/2})^{n_\tau}}{1+(\tau/\tau_{1/2})^{n_\tau}} \cdot \frac{RP_2}{T_\tau} \Theta \frac{2a_{RP}}{s}. \tag{1.10}$$

Thus, shear activation is 'spread' over the width of the whole transition zone. In equations (1.9), (1.10), τ is a scalar quantity equal to the magnitude of the stress tensor:

$$\tau = 0.01\eta\,\dot{\gamma}. \tag{1.11}$$

The factor 0.01 is introduced because the viscosity is measured in centipoises.

1.1.5. Generation of the activator by platelets. Platelets release ADP from their dense granules in their activation. We use the principle of the description of this process proposed previously in [48]. According to this principle, the rate of ADP production is proportional to the rate of platelets activation:

$$\begin{aligned} W_1^{\text{rel}} &= W_1^{\text{chem}}\,\lambda_{\text{ADP}} \\ W_2^{\text{rel}} &= \left(W_2^{\text{chem}} + W_2^{\text{stress}}\right)\lambda_{\text{ADP}}. \end{aligned} \tag{1.12}$$

Here λ_{ADP} is the quantity of ADP released from a single platelet. The ADP hydrolysis rate in the blood is equal to

$$W_{\text{ADP}}^{\text{hydr}} = \frac{V_m^{\text{hydr, ADP}} ADP}{K_m^{\text{hydr, ADP}} + ADP}. \tag{1.13}$$

1.2. Growth of a thrombocyte aggregate

In this paper we consider a quasi-two-dimensional formulation of the problem (see Fig. 2A), but the model can be directly extended to the three-dimensional case. The flow domain in our study was the rectangle $[-L_1 \leqslant x \leqslant L_2] \times [0 \leqslant y \leqslant L_3]$. The pressure value p_0 at the input was chosen so that at the initial time moment (in the absence of the thrombocyte aggregate) the near-wall shear rate was equal to the given value $\dot{\gamma}_{w,0}$:

$$p_0 = 2\dot{\gamma}_{w,0}\eta\,\frac{L_1+L_2}{L_3} \tag{1.14}$$

where η is the viscosity of blood. In order to trace the motion of the aggregate's boundary, the level set approach (LSA) has been used. In this method, the sharp

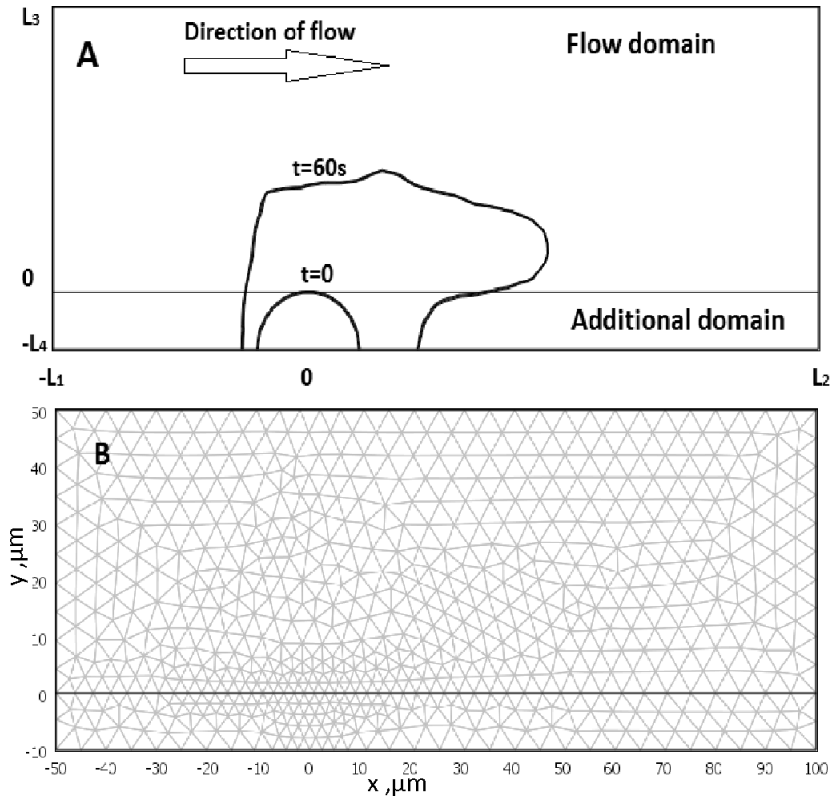

Figure 2. Calculation domain (A) and computational grid (B). All variables except for φ are determined in the upper rectangle $[-L_1 \leqslant x \leqslant L_2] \times [0 \leqslant y \leqslant L_3]$. The position $x = -L_1$ corresponds to the inlet, $x = L_2$ corresponds to the outlet, the values $y = 0$ and $y = L_3$ correspond to the walls impermeable to the flow. The function φ was defined in both rectangles $-L_4 \leqslant y \leqslant L_3$. The curve lines on the panel A are zero-level lines of the function φ and indicate the exact boundary of the thrombus at the beginning and at the end of a typical calculation.

boundary of the domain, where a jump of the physical properties of the medium occurs, is replaced by the transition zone of their continuous variation. The width s of this zone must be greater than the mesh size and much less than the typical size of the adjacent domains. In our case the mesh size in the thrombus zone was $1 \div 2\ \mu m$, the width of the flow was $50\ \mu m$, the diametrical size of the aggregate was $10 \div 40\ \mu m$. Therefore, the admissible width of the transition zone was about $2 \div 5\ \mu m$. Since the aggregate actually grows by capturing separate platelets whose diametrical size is of the order $2a_P = 2.4 \mu m$ and this growth is inhomogeneous over its surface, the boundary of the thrombus principally has a thickness not less that several micrometers. In the calculations the width s of the transition zone was taken equal to $2.5\ \mu m$. Below we describe the implementation of LSA in the model of platelets aggregation.

In order to identify the spatial domains forming the aggregate and the blood flow zone, we used the indicator function φ; its negative value means that a point

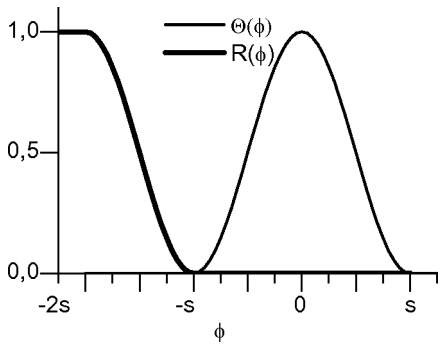

Figure 3. Structure of the transition zone. The distribution of adhesion, detachment, and shear activation processes is done according to the zone $-s < \varphi < s$ (where $\Theta(\varphi) > 0$). The aggregate resists the flow in the zone $\varphi < -s$ (where $R(\varphi) > 0$). This spatial distribution allows us to calculate correctly the shear rate in the zone of adhesion, i.e., in the zone $-s < \varphi < s$.

belongs to the aggregate, and a positive value corresponds to the blood flow. The line of zero level of φ (where $\varphi = 0$) is called the exact boundary of the aggregate. The value $|\varphi|$ indicates the distance from a given point of the surface, because in the process of calculation we try to keep $|\nabla\varphi|$ close to 1 in the transition zone and in its neighbourhood. This allows us to obtain easily the function Θ identifying the transition zone as the domain where $\Theta(\varphi) \geqslant 0$:

$$\Theta(\varphi) = H\left(\varphi + \frac{s}{2}, \frac{s}{2}\right) \cdot H\left(-\varphi + \frac{s}{2}, \frac{s}{2}\right). \tag{1.15}$$

Here the smoothed Heaviside function $H(r, r_0)$ serves as the trigger function H smoothly varying from 0 to 1 in the interval $-r_0 < r < r_0$. Therefore, $\Theta(\varphi) = 0$ for $|\varphi| \geqslant s$ and it is smoothly increased up to $\Theta(0) = 1$ when φ approaches 0 (see Fig. 3). For $|\nabla\varphi| = 1$ the dependence of Θ on the coordinate in the direction transversal to the surface, $\Theta(r)$, has a peak form with the width of the base equal to $2s$, the half-width (width at the half-height) equal to s, and the area s. For $s \to 0$ we have $\Theta(r)/s \to \delta(r)$.

The adhesion of each platelet changes the position of the boundary by the distance equal to the size of a platelet. The consideration of the balance of the number of platelets in the boundary layer easily implies that the velocity of the boundary is equal to

$$w = \left(W_{RP}^{\text{adh}} - W_{RP}^{\text{det}} + W_{AP}^{\text{adh}}\right) \frac{s}{P_m}. \tag{1.16}$$

The motion of the boundary occurs in the normal direction to it, which is determined in LSA as

$$\bar{n} = \frac{\nabla\varphi}{|\nabla\varphi|}. \tag{1.17}$$

The boundary velocity vector equals

$$\bar{w} = w\bar{n}. \tag{1.18}$$

In accordance with the LSA, in order to provide the motion of the boundary at this velocity, we have to solve the following convection equation, which is the Hamilton–Jacobi equation:

$$\frac{\partial \varphi}{\partial t} + \bar{w}\nabla\varphi = 0. \tag{1.19}$$

Taking into account equations (1.17) and (1.18), we have

$$\frac{\partial \varphi}{\partial t} + w|\nabla\varphi| = 0. \tag{1.20}$$

The diffusion and source terms are added to the right-hand side of (1.20) to stabilize the numerical solution of this equation and keep $|\nabla\varphi|$ close to 1:

$$\frac{\partial \varphi}{\partial t} + w|\nabla\varphi| = (\lambda\Delta\varphi + \beta S(\varphi)\,(1 - |\nabla\varphi|))\,\frac{\langle w\rangle}{w_0} \tag{1.21}$$

where $S(\varphi)$ is a continuous analogue of the function $\mathrm{sign}(\varphi)$:

$$S(\varphi) = \frac{\varphi}{\sqrt{\varphi^2 + (4s)^2}}. \tag{1.22}$$

The whole right-hand side of equation (1.21) is proportional to the mean velocity $\langle w\rangle$ of the boundary motion in order not to outweigh the convective term at the left-hand side of the equation. The parameters β and λ are chosen the minimum possible. The value λ should be of the order of the product of the boundary motion velocity and the mesh size. Since the thrombus growth rate in an arteriole is of order 1 μm/s and the mesh size is 2–4 μm, the base value of λ was 2 $\mu\mathrm{m}^2/\mathrm{s}$. The value of β was taken minimal, so that the value of $|\nabla\varphi|$ be close to 1 in the whole transition zone during the total calculation time.

For all boundaries of the computational domain of blood flow except for the lower one $(y = 0)$, the boundary condition for φ was specified in the form

$$\bar{n}\cdot\nabla\varphi = 0. \tag{1.23}$$

The conditions on the boundaries positioned far from the transition zone $(-s < \varphi < s)$ have a weak effect on the motion of the line $\varphi = 0$. However, this is not so for the boundary $y = 0$, because the line $\varphi = 0$ always crosses it. Therefore, the domain of definition of the function $\varphi(x,y)$ is extended to the additional rectangular domain having the width L_4 and adjacent to the lower boundary (see Fig. 2). The boundary $y = 0$ becomes internal for equation (1.21) and does not now require any boundary condition. The conditions on the outer boundaries of the additional domain had form (1.23). The transfer velocity of the level function in the additional domain $(y < 0)$ was equal to the value calculated on the boundary $y = 0$ for the same coordinate x.

In order to take into account the resistance of the aggregate to the flow, we added into the right-had side of the Navier–Stokes equations the term of the volume density of the force acting on the plasma filtered through it:

$$\bar{F} = -\frac{\eta_P}{K_D}\,\bar{u}R. \tag{1.24}$$

The domain of resistance of the aggregate to the flow was determined by the function R equal to 0 outside the aggregate and to 1 inside of it (see Fig. 3):

$$R(x,y) = H(-\varphi - 1.5s, 0.5s). \tag{1.25}$$

The coefficient of permeability in the sense of Darsy K_D was estimated under the assumption that the plasma is filtered trough the aggregate via cylindrical channels (viscosities η_P) and the profile of its velocity in each channel is parabolic. If the concentration of platelets in the aggregate is P_m, then a single platelet occupies approximately $l = 1/\sqrt[3]{P_m}$ of the channel's length. The resistance force to the fluid flow on a part of a channel of the length l and the diameter d is equal to

$$\bar{F}_1 = -\bar{\tau}_w(u,d)\,\pi d\,l = -8\pi\,\eta_P \bar{u} l \tag{1.26}$$

where $\tau_w(u,d)$ is the near-wall shear velocity in the channel, u is the mean plasma velocity in the channel equal to the macroscopic filtration rate. Therefore, inside the aggregate we have

$$\bar{F} \approx \bar{F}_1 P_m = -8\pi\eta_P \bar{u} P_m^{2/3} \tag{1.27}$$

which gives

$$K_D \approx \frac{1}{8\pi P_m^{2/3}}. \tag{1.28}$$

The growth kinetics of the aggregate is characterized in the model by the two following parameters: the total number of platelets in the aggregate (per unit thickness in the direction perpendicular to the plane xy), platelet/μm,

$$P_2(t) = \iint (RP_2 + AP_2)\,\mathrm{d}x\mathrm{d}y \tag{1.29}$$

and the area of its cross-section by the plane xy ('two-dimensional volume', i.e., the equivalent of the volume of a three-dimensional object), μm^2,

$$A(t) = \iint (\varphi < 0)\,\mathrm{d}x\mathrm{d}y. \tag{1.30}$$

The integration was performed over the whole blood flow domain ($y \geqslant 0$). We got $A(t) \approx P_2(t)/P_m$ in all the calculations.

1.3. Transport of erythrocytes and platelets

The blood was considered as a one-phase fluid with the constant density and viscosity (we neglected the difference in the densities of erythrocytes and the plasma because it is $\sim 7\%$ [34], and also the non-Newton properties of blood, because they become evident only for shear velocities $\sim 50\ \mathrm{s}^{-1}$ and lower [9, 24], whereas the typical shear velocities in microcirculation vessels are $(1 \div 2) \times 10^3\ \mathrm{s}^{-1}$ [27]). Therefore, the rate of convection of free erythrocytes and free platelets was assumed to be equal to the velocity of the medium. The platelets fixed in the aggregate were assumed to be motionless.

The shear-induced diffusion coefficients of erythrocytes and platelets moving in the flow are close or equal to each other (see [23, 57]). They were calculated from an analytical approximation of the results of a series of experimental measurements [57] as

$$\mathrm{D}_{\mathrm{ZC}} = kR_{RBC}^2 \frac{\dot{\gamma}_{w,0}}{2} \Phi_0 \left(1 - \Phi_0\right)^n. \tag{1.31}$$

Here R_{RBC} is the main radius of an erythrocyte, $\dot{\gamma}_{w,0}/2$ is the mean shear velocity, Φ_0 is the volume fraction of erythrocytes at the inflow (inflow hematocrit/100%), $kR_{RBC}^2 = 2.646\mu\mathrm{m}^2$, $n = 0.8$.

The distribution of erythrocytes across the blood flow is inhomogeneous: their volume portion is almost zero near the wall and is maximal on the axis of the flow. In a rectilinear flow this distribution has the form [50, 51]

$$\Phi_{RBC,0}(y) = \Phi_{RBC,m} \left[1 - \exp\left(a - b\Phi_{RBC,m}\right) + \exp\left(a - b\Phi_{RBC,m} \frac{4y(L_3 - y)}{L_3^2}\right)\right]^{-1}$$
$$\Phi_{RBC,m} = \frac{1.45\Phi_0}{0.5 + \Phi_0} \tag{1.32}$$

where $\Phi_{RBC,m}$ is the volume portion on the axis of the flow, $a = 3.5$ and $b = 9$ are constants. This formula was used for the determination of the initial and input distributions of erythrocytes. In order to support this inhomogeneity of the distribution and impermeability of erythrocytes into the thrombocyte aggregate, their dispersive flow was specified in the form

$$\bar{J}_{RBC}^D = -D\nabla\Phi_{RBC} + (1 - \Theta) D \Phi_{RBC} \nabla \ln \Phi_a^{RBC} \tag{1.33}$$

where

$$\Phi_a^{RBC} = \Phi_{RBC,0}(y) \exp\left[-4\mathrm{R}(\varphi)\right].$$

Equation (1.33) gives $\Phi_{RBC}(x,y) \sim \Phi_a^{RBC}(x,y)$ in the stationary mode. In order to balance the concentration of erythrocytes across the transition zone, the factor $(1 - \Theta)$ was added into equation (1.33) and an artificial flow was added into transport equation (A6), which was directed perpendicular to the transition zone and was nonzero only in that zone:

$$\bar{J}_{RBC}^{\Theta} = \Theta \cdot (-100 D \nabla \Phi_{RBC}, \bar{n}) \cdot \bar{n}. \tag{1.34}$$

The boundary condition on the walls of the vessel and at the outflow has the form $\bar{n}_{\text{bound}}\left(\bar{J}^{D}_{RBC}+\bar{J}^{\Theta}_{RBC}\right)=0$.

The distribution of platelets across the flow is also inhomogeneous, they are displaced by erythrocytes from the centre of the flow to the walls. The local portion of the volume available for platelets is generally determined by the volume portion of erythrocytes [13,50]. It is approximately equal to $\exp\left[-2\Phi_{RBC}\left(1+2\Phi_{RBC}\right)\right]$ [50]. In order to prevent the penetration of platelets carried by the blood flow into the thrombus deeper than the transition zone, this expression was multiplied by the following function quickly decreasing for $\varphi<-s$:

$$\Phi^{P}_{a}=\exp\left[-2\Phi_{RBC}\left(1+2\Phi_{RBC}\right)\right]\exp\left[-4\mathrm{R}(\varphi)\right]. \tag{1.35}$$

The flows of platelets had the form

$$\begin{aligned}\bar{J}^{D}_{RP1}&=-D\nabla RP_1+(1-\Theta)\,D\cdot RP_1\cdot\nabla\ln\Phi^{P}_{a}\\ \bar{J}^{D}_{AP1}&=-D\nabla AP_1+(1-\Theta)\,D\cdot AP_1\cdot\nabla\ln\Phi^{P}_{a}.\end{aligned} \tag{1.36}$$

The initial and input distribution of nonactivated platelets were specified proportional to the initial profile of Φ_a [50]:

$$RP_1(y)_{t=0}=P_0\frac{\Phi^{P}_{a}(\Phi_{RBC,0}(y))}{\bar{\Phi}^{P}_{a}} \tag{1.37}$$

where P_0 is the mean concentration of platelets in the blood, $\bar{\Phi}^{P}_{a}$ is the mean volume portion accessible for platelets in the cross-section of the vessel. In order to balance the concentration of platelets across the transition zone, we introduced the factor $(1-\Theta)$ into the right-hand side of equation (1.36) and add the following artificial flows into transport equations (A1)–(A4):

$$\begin{aligned}\bar{J}^{\Theta}_{RP1}&=\left(-(100D+100D_{\text{adh}})\nabla RP_1,\bar{n}\right)\bar{n}\,\Theta\\ \bar{J}^{\Theta}_{AP1}&=\left(-(100D+100D_{\text{adh}})\nabla AP_1,\bar{n}\right)\bar{n}\,\Theta\end{aligned} \tag{1.38}$$

The coefficients $100D$ and $100D_{\text{adh}}$ are taken to balance the gradients created by flows (1.36) and the adhesion of platelets, respectively, over the transition zone. Here $D_{\text{adh}}=(2s)^2/(2t_{\text{adh}})$, $t_{\text{adh}}\sim\left(\alpha K\dot{\gamma}\Phi_{RBC}/s\right)^{-1}$ is the typical adhesion time (see equations (1.1), (1.4)). The boundary conditions for platelets on the walls of the vessel and at the outflow had the form $\bar{n}_{\text{bound}}\left(\bar{J}^{D}_{P}+\bar{J}^{\Theta}_{P}\right)=0$.

1.4. Numerical methods

The equations of the model (see Appendix A) was solved by the package COMSOL Multiphysics 3.4 using the finite element method with second-order Lagrange elements for the function φ and concentrations of platelets and ADP. Solving the Navier–Stokes equations, we used second-order elements for the velocities and linear ones for the pressure. The computation grid is shown in Fig. 2B. The accuracy of calculations was 1%.

2. Results

2.1. General pattern of the growth of a thrombus in a blood flow

For the sake of simplicity, in this paper we take into account only the basic soluble activator of platelets, ADP, because the other activators (thrombin and thromboxane A_2) are considered similarly [20, 29, 48]. Therefore, we have used the results of [3] for a direct comparison with the experiment. In this paper, the growth of a thrombus was activated by an injection of ADP into the wall of a venule of the cheek pouch of a hamster. The typical results of the calculations simulating these experiments are presented in Fig. 4B (Fig. 4A corresponds to $t = 0$). The gradations of grey indicate the total concentration of aggregated platelets. It is seen that the thrombus is formed locally near the activation place. In the course of time, its growth spreads in all directions with the increasing downstream tendency due to the drift of the activator caused by the flow. This character of the growth is in accordance with the experimental data *in vivo* both in the statement of [3] (panel C) and in the laser model of the thrombosis of mice [18] (panel D).

The lines in Figs. 4A and 4B indicate the 'blurred' (distributed) boundary of the aggregate, the levels $-s$, 0, and s of the function φ. The width of the transition zone remained constant and close to $2s$ in the whole process of calculation. The velocity field is shown by the arrows. The flow goes around the growing aggregate, and only slow plasma filtration occurs in the zone $\varphi < -s$. These results show that we have succeeded in the solution of the fluid-structure interaction problem under a continuous variation of the size and form of the body resisting the flow, and also indicate that the proposed variant of LSA is well applicable to problems of this kind.

2.2. Dependence of the thrombus growth rate on the near-wall shear velocity

The near-wall shear velocity is the main parameter determining the influence of the flow on the thrombocyte components of hemostasis, because it controls the delivery rate of platelets to the point of adhesion and their detachment by the flow and also the velocity of the convective drift of thrombocyte activators. Therefore, we have studied the influence of shear velocity on the thrombus growth rate in our model. Figure 5A shows the kinetics of accumulation of aggregated platelets for different shear velocities. The increase in the shear velocity causes a proportional increase in the accumulation rate. Beginning with the time moment ~ 20 s, the curves take an exponential form and are straightened in the semilogarithmic coordinates (see Fig. 5B). We had calculated the efficient 'thrombus growth rate constant' from the incline of the linear parts of these curves in the same way as this was done in experimental study [3]. It occurs that the dependence of the efficient growth rate constant on the shear velocity has a sharp maximum positioned in the shear velocity range $50 \div 100\,\mathrm{s}^{-1}$ (see Fig. 5C). These shear velocities correspond to the mean flow velocities $400 \div 800\mu$m/s. A similar dependence was obtained in the experiment (see Fig. 5D) with the only difference that its form was more sharp and the maximum was localized near 300μm/s.

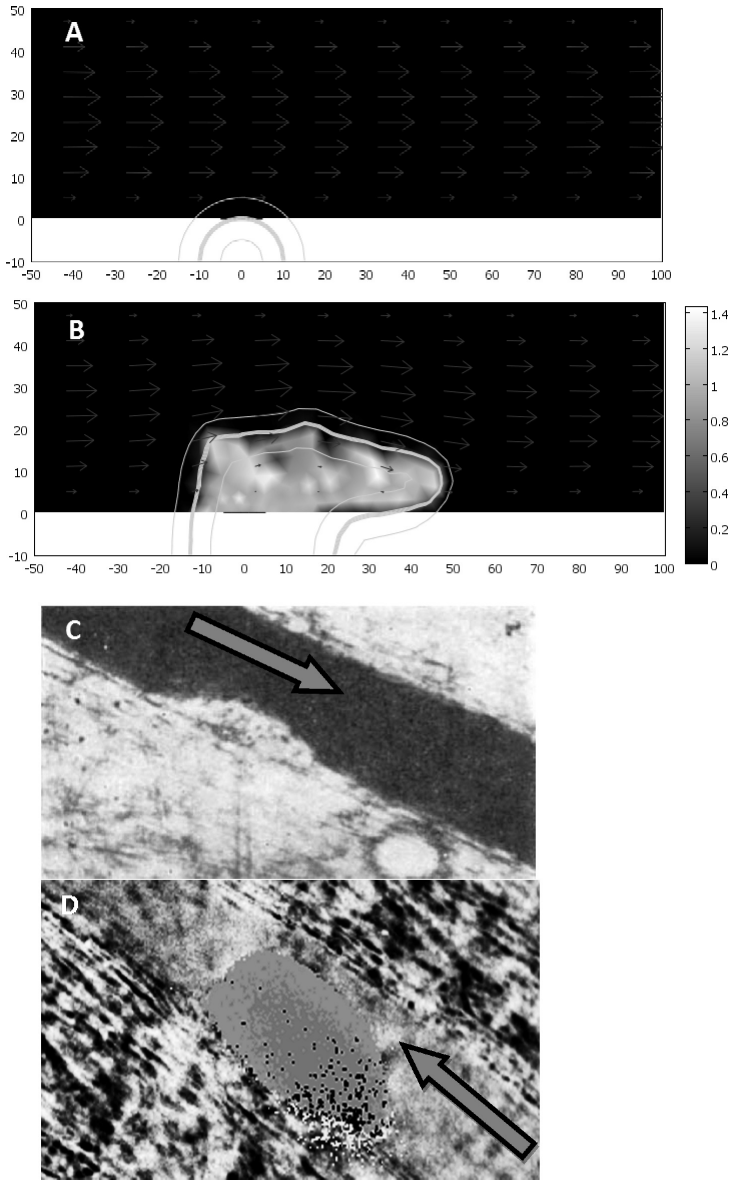

Figure 4. Typical pattern of the growth of a thrombocyte thrombus in a blood flow in the model (A,B) and *in vivo* (C,D). (A,B) The total concentration of platelets in the aggregate p_2 (grey), the isolines $\varphi = -s, 0, s$ (curves), and the flow velocity field (arrows) are shown for the time moments $t = 0$ (A) and 60 s (B). The near-wall shear velocity is 800 s^{-1}, all other parameters are indicated in Table 1. The black segment on the boundary $y = 0$ near $x = 0$ marks the ADP inflow zone. The calculation time was approximately 280 hours. (C) The growth of a thrombus in a venule of the cheek pouch of a hamster ($d = 40 \div 70 \mu$m) was initialed by the iontophoretic injection of ADP through a micropipette [3]. (D) The growth of a thrombus in an arteriole of a mouse ($d = 40 \div 60 \mu$m) was initiated by injuring the wall by a laser [18]. The arrows in C and D show the direction of the blood flow.

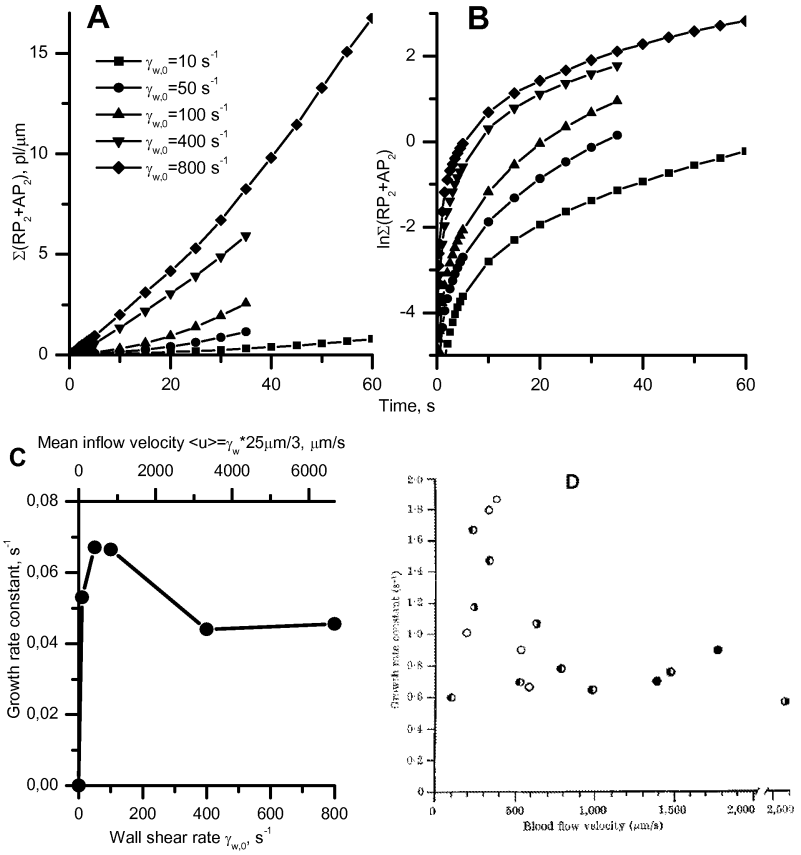

Figure 5. Kinetics of the growth of a thrombocyte thrombus. (A,B) The dependence of the total number of platelets in the thrombus on time for different near-wall shear velocities in linear and semilogarithmic coordinates. (C) The thrombus growth rate constant calculated from the incline of the curves from panel B on the period $t = 20 \div 35$ s. The upper axis is obtained from the lower one by the multiplication by $L_3/6$ and is presented for comparison with panel D. (D) The experimental thrombus growth rate constant calculated from the kinetics of its volume [3].

3. Conclusion

The aim of this paper was the development of a continuous PDE-based numerical model of the thrombocyte component of hemostasis taking into account all its basic processes, such as the transport of platelets along and across the blood flow, their adhesion to the injured place of a vascular wall and to the surface of a growing thrombocyte aggregate, the activation, the emission of activators, and the aggregation of platelets. The main difficulty was in the description of the process of the thrombocyte aggregate growth into the blood flow occurring due to the adhesion of platelets carried by the flow. This is caused by the principal nonlocality of the adhesion (a finite size of platelets) and by the necessity to calculate the rate of this process on the moving boundary of the aggregate. Along with the description of all basic processes of the thrombocyte component of the hemostasis, an advantage

of the model constructed here is its flexibility and its ability to be integrated into continuous models of blood flow in domains with a complex geometry and with fixed [4, 14, 30, 42] or moving walls [44, 46, 54], and also for the whole vascular network. A network of vessels can be described by a multiscale model combining (a) one-dimensional flows of the Poiseuille type in regular parts with parallel walls and without obstacles and (b) two-dimensional Navier–Stokes description in the zones of a more complicated geometry: bifurcations and clot formation areas [8, 39]. In addition, this model can be easily supplemented with differential equations describing the action of all the three activators of platelets [20, 29, 48] and the work of the plasma coagulation system [40, 41]. This produces a sufficiently complete quantitative model of hemostasis applicable to the study of its regulation and mechanisms of transitions from normal functioning to a pathologic behaviour, such as hemorrhaging and thrombosis.

This work is a part of the joint French-Russian Programme International de Cooperation Scientifique (PICS CNRS) 'Mathematical modelling of blood diseases'. It was partly supported by the Russian Foundation for Basic Research (09–04–00232, 10–01–91055, and 11–04–00303), by grant 14.740.11.0875 'Multiscale problems: analysis and methods' of the Ministry of Education and Research of the Russian Federation and by SFR MOMAD of the University of Saint Etienne and ENISE (the Ministry of Research and Education of France).

Appendix A. Differential equations of the model

Dimensionality: t: s; x, y: μm; RP_1, AP_1, RP_2,AP_2: platelet/μm^3; W_{RP}^{adh}, W_{AP}^{adh}, W_{RP}^{det}, W_1^{chem}, W_2^{chem}, W_2^{stress}: platelet/μm$^3\cdot$ s; J_{RP}^{wall}, J_{AP}^{wall}, $\left|J_{RP1}^{D}\right|$, $\left|J_{RP1}^{\Theta}\right|$, $\left|J_{AP1}^{D}\right|$, $\left|J_{AP1}^{\Theta}\right|$: platelet/$\mu$m$^2\cdot$ s; ADP: nm; W_1^{rel}, W_2^{rel}, $W_{\mathrm{ADP}}^{\mathrm{hydr}}$: nm/s; $\bar{u}$: μm/s; $\dot{\gamma}$: 1/s; τ, p: dyne/cm^2; $\bar{F}$: μg/μm$^2\cdot$s$^2 = 10^{-18}$ N/μm^3); $P_2(t)$: platelet/μm; $A(t)$: μm^2.

Kinetics and transport of platelets:

$$\frac{\partial}{\partial t}RP_1 + (\bar{u}\nabla)\,RP_1 = -\nabla\left(\bar{J}_{RP1}^{D} + \bar{J}_{RP1}^{\Theta}\right) - \left(W_{RP}^{\mathrm{adh}} - W_{RP}^{\mathrm{det}} + W_1^{\mathrm{chem}}\right) \tag{A1}$$

$$\frac{\partial}{\partial t}AP_1 + (\bar{u}\nabla)\,AP_1 = -\nabla\left(\bar{J}_{AP1}^{D} + \bar{J}_{AP1}^{\Theta}\right) + \left(W_1^{\mathrm{chem}} - W_{AP}^{\mathrm{adh}}\right) \tag{A2}$$

$$\frac{\mathrm{d}}{\mathrm{d}t}RP_2 = \left(W_{RP}^{\mathrm{adh}} - W_{RP}^{\mathrm{det}}\right) - \left(W_2^{\mathrm{chem}} + W_2^{\mathrm{stress}}\right) \tag{A3}$$

$$\frac{\mathrm{d}}{\mathrm{d}t}AP_2 = W_2^{\mathrm{chem}} + W_2^{\mathrm{stress}} + W_{AP}^{\mathrm{adh}} \tag{A4}$$

Kinetics and transport of ADP:

$$\frac{\partial}{\partial t}ADP + (\bar{u}\nabla)\,ADP = D_{\mathrm{ADP}}\Delta ADP + W_1^{\mathrm{rel}} + W_2^{\mathrm{rel}} - W^{\mathrm{hydr}}. \qquad (A5)$$

Transport of erythrocytes:

$$\frac{\partial}{\partial t}\Phi_{RBC} + (\bar{u}\nabla)\,\Phi_{RBC} = -\nabla\left(\bar{J}_{RBC}^{D} + \bar{J}_{RBC}^{\Theta}\right). \qquad (A6)$$

Equations of fluid flow (Navier–Stokes equations):

$$\nabla \cdot \bar{u} = 0 \qquad (A7)$$

$$\rho\frac{\partial}{\partial t}\bar{u} + \rho\,(\bar{u}\nabla)\,\bar{u} = \nabla\left(-p\bar{\bar{I}} + 2\eta\bar{\bar{S}}\right) + \bar{F} \qquad (A8)$$

$$\bar{\bar{S}} = \frac{1}{2}\left(\nabla\bar{u} + (\nabla\bar{u})^{T}\right). \qquad (A9)$$

Motion of aggregate (thrombus) boundary:

$$\frac{\partial\varphi}{\partial t} + w\,|\nabla\varphi| = \left(\lambda\Delta\varphi + \beta\cdot S(\varphi)\,(1 - |\nabla\varphi|)\right)\langle w\rangle. \qquad (A10)$$

References

1. P. A. Aarts, S. A. van den Broek, G. W. Prins, G. D. Kuiken, J. J. Sixma, and R. M. Heethaar, Blood platelets are concentrated near the wall and red blood cells, in the center in flowing blood. *Arteriosclerosis* (1988) **8**, No. 6, 819–824.
2. D. Adalsteinsson and J. A. Sethian, A fast level set method for propagating interfaces. *J. Comp. Phys.* (1995) **118**, No. 2, 269–277.
3. N. Begent and G. V. Born, Growth rate in vivo of platelet thrombi, produced by iontophoresis of ADP, as a function of mean blood flow velocity. *Nature* (1970) **227**, No. 5261, 926–930.
4. D. Bluestein, L. Niu, R. T. Schoephoerster, and M. K. Dewanjee, Steady flow in an aneurysm model: correlation between fluid dynamics and blood platelet deposition. *J. Biomech. Eng.* (1996) **118**, No. 3, 280–286.
5. J. P. Bossavy, K. S. Sakariassen, A. Barret, B. Boneu, and Y. Cadroy, A new method for quantifying platelet deposition in flowing native blood in an ex vivo model of human thrombogenesis. *Thromb. Haemost.* (1998) **79**, No. 1, 162–168.
6. J. P. Bossavy, K. S. Sakariassen, C. Thalamas, B. Boneu, and Y. Cadroy, Antithrombotic efficacy of the vitamin K antagonist fluindione in a human ex vivo model of arterial thrombosis: effect of anticoagulation level and combination therapy with aspirin. *Arterioscler. Thromb. Vasc. Biol.* (1999) **19**, No. 9, 2269–2275.
7. J. P. Bossavy, C. Thalamas, L. Sagnard, A. Barret, K. Sakariassen, B. Boneu, and Y. Cadroy, A double-blind randomized comparison of combined aspirin and ticlopidine therapy versus aspirin or ticlopidine alone on experimental arterial thrombogenesis in humans. *Blood* (1998) **92**, No. 5, 1518–1525.

8. G. Cardone, G. Panasenko, and I. Sirakov, Asymptotic analysis and numerical modelling of mass transport in tubular structure. arXiv: 0910. 5683v2, (2009).

9. C. G. Caro, T. J. Pedley, R. C. Schroter, and W. A. Seed, *The Mechanics of the Circulation*. Cambridge Univ. Press, Cambridge–New York, 2012.

10. T. W. Chow, J. D. Hellums, J. L. Moake, and M. H. Kroll, Shear stress-induced von Willebrand factor binding to platelet glycoprotein Ib initiates calcium influx associated with aggregation. *Blood* (1992) **80**, No. 1, 113–120.

11. S. B. Coade and J. D. Pearson, Metabolism of adenine nucleotides in human blood. *Circ. Res.* (1989) 65, 531–537.

12. R. W. Colman, A. W. Clowes, S. Z. Goldhaber, V. J. Marder, and J. N. George, *Hemostasis and Thrombosis-Basic Principles and Clinical Practice*. Lippincott Williams & Wilkins, 2006.

13. L. Crowl and A. L. Fogelson, Analysis of mechanisms for platelet near-wall excess under arterial blood flow conditions. *J. Fluid Mech.*, Available on CJO 2006 (2011).

14. B. Das, G. Enden, and A. S. Popel, Stratified multiphase model for blood flow in a venular bifurcation. *Annals Biomed. Eng.* (1997) **25**, 135–153.

15. T. E. Diller, Comparison of red cell augmented diffusion and platelet transport. *J. Biomech. Eng.* (1988) **110**, No. 2, 161–163.

16. E. C. Eckstein and F. Belgacem, Model of platelet transport in flowing blood with drift and diffusion terms. *Biophys. J.* (1991) **60**, No. 1, 53–69.

17. E. C. Eckstein, D. L. Bilsker, C. M. Waters, J. S. Kippenhan, and A. W. Tilles, Transport of platelets in flowing blood. *Ann. N.Y. Acad. Sci.* (1987) **516**, 442–452.

18. S. Falati, P. Gross, G. Merrill-Skoloff, B. C. Furie, and B. Furie, Real-time in vivo imaging of platelets, tissue factor and fibrin during arterial thrombus formation in the mouse. *Nat. Med.* (2002) **8**, No. 10, 1175–1181.

19. A. L. Fogelson and R. D. Guy, Platelet-wall interactions in continuum models of platelet thrombosis: formulation and numerical solution. *Math. Med. Biol.* (2004) **21**, No. 4, 293–334.

20. B. J. Folie and L. V. McIntire, Mathematical analysis of mural thrombogenesis. Concentration profiles of platelet-activating agents and effects of viscous shear flow. *Biophys. J.* (1989) **56**, No. 6, 1121–1141.

21. M. M. Frojmovic, R. F. Mooney, and T. Wong, Dynamics of platelet glycoprotein IIb-IIIa receptor expression and fibrinogen binding. I. Quantal activation of platelet subpopulations varies with adenosine diphosphate concentration. *Biophys. J.* (1994) **67**, No. 5, 2060–2068.

22. M. M. Frojmovic, R. F. Mooney, and T. Wong, Dynamics of platelet glycoprotein IIb-IIIa receptor expression and fibrinogen binding. II. Quantal activation parallels platelet capture in stir-associated microaggregation. *Biophys. J.* (1994) **67**, No. 5, 2069–2075.

23. H. L. Goldsmith, Red cell motions and wall interactions in tube flow. *Fed. Proc.* (1971) **30**, No. 5, 1578–1590.

24. H. L. Goldsmith and V. T. Turitto, Rheological aspects of thrombosis and haemostasis: basic principles and applications. ICTH-Report–Subcommittee on Rheology of the International Committee on Thrombosis and Haemostasis. *Thromb. Haemost.* (1986) **55**, No. 3, 415–435.

25. P. D. Goodman, E. T. Barlow, P. M. Crapo, S. F. Mohammad, and K. A. Solen, Computational model of device-induced thrombosis and thromboembolism. *Ann. Biomed. Eng.* (2005) **33**, No. 6, 780–797.

26. R. R. Hantgan, A study of the kinetics of ADP-triggered platelet shape change. *Blood* (1984) **64**, No. 4, 896–906.

27. J. J. Hathcock, Flow effects on coagulation and thrombosis. *Arterioscler. Thromb. Vasc. Biol.* (2006) **26**, No. 8, 1729–1737.

28. M. Hofer and K. Perctold, Computer simulation of concentrated fluid-particle suspension flows in axisymmetric geometries. *Biorheology* (1997) **54**, No. 4/5, 261–279.

29. J. A. Hubbell and L. V. McIntire, Platelet active concentration profiles near growing thrombi. A mathematical consideration. *Biophys. J.* (1986) **50**, No. 5, 937–945.

30. J. Jung and A. Hassenein, Three-phase CFD analytical modelling of blood flow. *Medical Engineering & Physics* (2008) **30**, 91–103.

31. S. Kulkarni, S. M. Dopheide, C. L. Yap, C. Ravanat, M. Freund, P. Mangin, K. A. Heel, A. Street, I. S. Harper, F. Lanza, and S. P. Jackson, A revised model of platelet aggregation. *J. Clin. Invest.* (2000) **105**, No. 6, 783–791.

32. N. Lantz, B. Hechler, C. Ravanat, J. P. Cazenave, and C. Gachet, A high concentration of ADP induces weak platelet granule secretion independently of aggregation and thromboxane A2 production. *Thromb. Haemost.* (2007) **98**, No. 5, 1145–1147.

33. K. Leiderman and A. L. Fogelson, Grow with the flow: a spatial-temporal model of platelet deposition and blood coagulation under flow. *Math. Med. Biol.* (2010) **28**, No. 1, 47–84.

34. V. A. Levtov, S. A. Regirer, and N. Ch. Shadrina, *Blood Rheology*. Medicine, Moscow, 1982 (in Russian).

35. J. L. Moake, N. A. Turner, N. A. Stathopoulos, L. Nolasco, and J. D. Hellums, Shear-induced platelet aggregation can be mediated by vWF released from platelets, as well as by exogenous large or unusually large vWF multimers, requires adenosine diphosphate, and is resistant to aspirin. *Blood* (1988) **71**, No. 5, 1366–1374.

36. N. A. Mody, O. Lomakin, T. A. Doggett, T. G. Diacovo, and M. R. King, Mechanics of transient platelet adhesion to von Willebrand factor under flow. *Biophys. J.* (2005) **88**, No. 2, 1432–1443.

37. P. Neofytou, Comparison of blood rheological models for physiological flow simulation. *Biorheology* (2004) **41**, No. 6, 693–714.

38. S. Osher and J. A. Sethian, Fronts propagating with curvature-dependent speed. *J. Comp. Phys.* (1988) **79**, 12–49.

39. G. P. Panasenko, Asymptotic expansion of the solution of Navier-Stokes equation in tube structure and partial asymptotic decomposition of the domain. *Applic. Anal. Int. J.* (2000) **76**, No. 3–4, 363–381.

40. M. A. Panteleev, A. N. Balandina, E. N. Lipets, M. V. Ovanesov, and F. I. Ataullakhanov, Task-oriented modular decomposition of biological networks: trigger mechanism in blood coagulation. *Biophys. J.* (2010) **98**, No. 9, 1751–1761.

41. M. A. Panteleev, M. V. Ovanesov, D. A. Kireev, A. M. Shibeko, E. I. Sinauridze, N. M. Ananyeva, A. A. Butylin, E. L. Saenko, and F. I. Ataullakhanov, Spatial propagation and localization of blood coagulation are regulated by intrinsic and protein C pathways, respectively. *Biophys. J.* (2006) **90**, No. 5, 1489–1500.

42. K. Perktold, M. Hofer, G. Rappitsch, M. Loew, B. D. Kuban, and M. H. Friedman, Validated computation of physiologic flow in a realistic coronary artery branch. *J. Biomech.* (1998) **31**, No. 3, 217–228.

43. A. S. Popel and P. C. Johnson, Microcirculation and hemorheology. *Annu. Rev. Fluid Mech.* (2005) **37**, 43–69.

44. A. M. Quarteroni, M. Tuveri, and A. Veneziani, Computational vascular fluid dynamics: problems, models and methods. *Computing and Visualization in Science* (2000) **2**, 163–197.

45. Z. M. Ruggeri and G. L. Mendolicchio, Adhesion mechanisms in platelet function. *Circ. Res.* (2007) **100**, No. 12, 1673–1685.

46. C. M. Scotti, J. Jimenez, S. C. Muluk, and E. A. Finol, Wall stress and flow dynamics in abdominal aortic aneurysms: finite element analysis vs. fluid-structure interaction. *Comp. Methods Biomech. Biomed. Eng.* (2008) **11**, No. 3, 301–322.

47. R. D. Smyth and W. G. Owen, Platelet responses to compound interactions with thrombin. *Biochemistry* (1999) **38**, 8936–8947.

48. E. N. Sorensen, G. W. Burgreen, W. R. Wagner, and J. F. Antaki, Computational simulation of platelet deposition and activation: I. Model development and properties. *Ann. Biomed. Eng.* (1999) **27**, No. 4, 436–448.

49. A. A. Tokarev, A. A. Butylin, and F. I. Ataullakhanov, Platelet adhesion from shear blood flow is controlled by near-wall rebounding collisions with erythrocytes. *Biophys. J.* (2011) **100**, No. 4, 799-808.

50. A. A. Tokarev, A. A. Butylin, E. A. Ermakova, E. E. Shnol, G. P. Panasenko, and F. I. Ataullakhanov, 'Excluded and available volumes' effect causes a strong non-uniform distribution of platelets across blood flow. *Biophys. J.* (2011) **101**, No. 8, 1835–1843.

51. A. Tokarev, G. Panasenko, and F. Ataullakhanov, Segregation of flowing blood: mathematical description. *Math. Modelling Natur. Phenom.* (2011) **6**, 281–319.

52. D. Varga-Szabo, I. Pleines, and B. Nieswandt, Cell adhesion mechanisms in platelets. *Arterioscler. Thromb. Vasc. Biol.* (2008) **28**, No. 3, 403–412.

53. J. L. N. Wolfs, P. Comfurius, J. T. Rasmussen, J. F. W. Keuren, T. Lindhout, R. F. A. Zwaal, and E. M. Bevers, Activated scramblase and inhibited aminophospholipid translocase cause phosphatidylserine exposure in a distinct platelet fraction. *Cell. Mol. Life Sci.* (2005) **62**, 1514–1525.

54. B. J. B. M. Wolters, M. C. M. Rutten, G. W. H. Schurink, U. Kose, J. D. Hart, and F. N. V. D. Vosse, A patient-specific computational model of fluid-structure interaction in abdominal aortic aneurysms. *Med. Eng. & Phys.* (2005) **27**, 871–883.

55. Y. P. Wu, P. G. de Groot, and J. J. Sixma, Shear-stress-induced detachment of blood platelets from various surfaces. *Arterioscler. Thromb. Vasc. Biol.* (1997) **17**, No. 11, 3202–3207.

56. C. Yeh, A. C. Calvez, and E. C. Eckstein, An estimated shape function for drift in a platelet-transport model. *Biophys. J.* (1994) **67**, No. 3, 1252–1259.

57. A. L. Zydney and C. K. Colton, Augmented solute transport in the shear flow of a concentrated suspension. *PCH PhysicoChem. Hydrodynam.* (1988) **10**, No. 1, 77–96.